Review of Zero-Emission Utah State Snowmobile (ZEUS)

Mathew Brown
Amanda Calder
Mark Fairbanks
Jeff Ferrin
Sam Francis
James Gyllenskog
Kyle Hanson
Ashley Kelly
Paul Overdiek
Daniel Plaizier
Utah State University Electric Snowmobile Team

ABSTRACT

This engineering design paper discusses the conversion of a stock 2005 Yamaha Vector snowmobile into a zero-emission vehicle in preparation for SAE's Clean Snowmobile Challenge.

INTRODUCTION

The design of Utah State University's zero-emission snowmobile (ZEUS) for the March 2007 SAE Clean Snowmobile Challenge focused on incorporating the benefits of a gas sled into a zero-emission configuration. The benefits of gas sleds are: acceleration, handling characteristics, range, reliability, rider comfort, safety, and weight.

Designing a zero-emission sled with these characteristics requires newer technologies in efficiency, energy storage, and weight reduction. In the design and production of ZEUS, the electric snowmobile team had to compromise the benefits of gas sleds and overall cost, as newer technologies are generally more expensive. The main constraint of this team was its budget. Most of the components were either inherited or donated, including the chassis, motor, and controller. Other design considerations, such as battery selection, were heavily weighted on the cost. An advantage of this constraint, however, is the MSRP of ZEUS is comparable to the stock sled.

The Clean Snowmobile Challenge, sponsored by SAE, encourages students to develop a cleaner and quieter snowmobile. The events test the snowmobile design to determine how it will perform in the real world. The first event examines the range of the sled. The competition requires that an electric sled have a range of 10 miles while averaging 20 mph. The next test is the cold start to determine if the sled can actually perform after being left in the cold overnight. With noise laws changing, SAE performs a noise test to make sure that the modified sleds are within the new requirements that will be enforced in the near future. The judges also do a subjective handling test. They furthermore test it for rider comfort with an accelerometer. All electrical sleds are then subjected to a draw-bar test. This event challenges the utility of the snowmobile by having it pull 1500 lbf over 100 ft. The final day of the competition, the sleds are subjected to an acceleration test and also an objective handling course. Each event is individually scored.

MAIN SECTION

The global characteristics that were designed to are: acceleration, handling characteristics, noise, range, reliability, rider comfort, safety, and weight. Each team's analysis and nomenclature are listed below.

NOMENCLATURE

a	=	*upper A-arm length*
A	=	*intermediate kinematic analysis constant*
$Area$	=	*surface area*
b	=	*spindle length*
B	=	*intermediate kinematic analysis constant*
Bi	=	*Biot number*
c	=	*lower A-arm length*
C	=	*intermediate kinematic analysis constant*
c_1	=	*constant: conversion from kWh to lb*ft*
c_2	=	*constant: conversion from mph to ft/sec*
c_3	=	*constant: conversion from ft to miles*
c_4	=	*constant based on Biot number*
d	=	*frame connection length*

D = *intermediate kinematic analysis constant*
d_{ft} = *distance that sled will travel in ft*
d = *distance that sled will travel in miles*
d_{equiv} = *equivalent diameter of track in ft*
E_{gen} = *energy generated in control volume*
E_{in} = *energy into control volume*
E_{out} = *energy coming out of control volume*
E_{st} = *energy stored in control volume*
E_0 = *zero-load battery voltage*
F = *drive force*
Fo - *Fourier number*
g = *gravitational constant*
h = *elevation increase*
h_{conv} = *convection coefficient*
I = *current draw*
J = *mass moment of inertia*
J_{equiv} = *equivalent mass moment of inertia*
K = *thermal conductivity*
L = *characteristic length*
L_{sled} = *load of the sled on rear suspension*
m = *mass of the sled and rider in slugs*
q_{tot} = *total heat energy*
R_b = *internal resistance of batteries*
R_{bequiv}= *equivalent resistance of battery pack*
R_{cAL} = *conduction resistance for aluminum*
R_{cf} = *conduction resistance for foam*
R_{cv} = *convection resistance*
R_g = *gear ratio of direct-drive system*
R_{ms} = *gear ratio of motor to secondary*
RPM = *revolutions per minute of the motor*
RR = *rolling resistance of sled in pounds*
R_{tot} = *total resistance*
R_{sc} = *gear ratio of secondary to cogs*
R_T = *radius of driving wheel*
t = *time in seconds*
T_i = *temperature of battery box at time i*
T_∞ = *ambient temperature*
T_0 = *initial temperature of battery box*
T_{0Eng} = *total battery energy in lb*ft*
T_{0Si} = *total battery energy in kWh*
x' = *distance traveled by sled*
x'' = *sled velocity*
$x^{\cdot}$ = *sled acceleration*
V_{mph} = *velocity in mph*
V_{fts} = *velocity in ft/sec*
W_{rider} = *weight of the rider*
α = *thermal diffusivity in m**2/s*
δ_c = *compressed rear-link length*
δ_f = *uncompressed rear-link length*
ζ_1 = *constant based on Biot number*
η_b = *efficiency of battery*
η_c = *efficiency of controller*
η_m = *efficiency of motor*
η_t = *efficiency of transmission*
η_{Tot} = *total efficiency of components*
θ' = *angle of cogs*
θ'' = *angular velocity of cogs*
$\theta^{\cdot}$ = *angular acceleration of cogs*
θ_{s_*} = *kinematic analysis angle*
θ_0 = *dimensionless temperature*
θ_2 = *kinematic analysis angle*
θ_3 = *kinematic analysis angle*
θ_4 = *kinematic analysis angle*
τ_c = *torque at cogs*
τ_{cs} = *torque of compressed stock spring*
τ_M = *motor torque*
τ_{0f} = *torque needed to keep sled at stock height*
φ_c = *compressed angle from vertical to link*
φ_f = *uncompressed angle from vertical to link*

CHASSIS

The chassis team's main considerations were handling characteristics, rider comfort, and structural safety. There were three major areas of the sled that the chassis team analyzed for modifications. These areas are the battery box and the front and rear suspensions.

Battery Box

ZEUS had to be redesigned to include a battery box in order to accommodate the placement of the twelve lead-acid batteries. The location of this battery box follows the 2005-2006 electric snowmobile team's design of a battery box that doubles as the rider's seat. This was a practical decision because various components that were previously under the seat such as the gas tank were no longer necessary.

Besides the competition requirements that the battery box be sealed, vented and nonconductive three main considerations were taken into account for the design of the battery box: battery layout, structural integrity, and thermal analysis. These considerations were based on the goals of handling characteristics, rider comfort, and the cold-start event.

Battery Layout

The center of gravity was the main concern of the battery layout. This is because battery weight accounts for approximately half of the weight of the sled. The further forward the center of gravity is placed, the closer the handling characteristics will parallel those of the stock sled. The chosen battery layout is shown below.

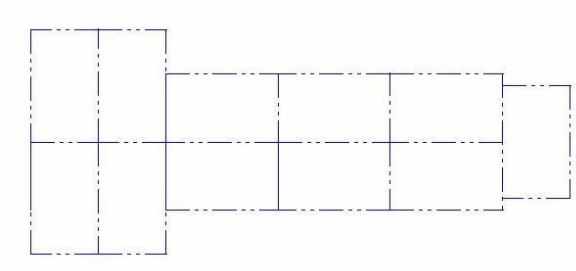

Figure 1: Battery layout

In designing the battery layout the batteries were placed to move the center of gravity as far forward as possible while still providing a comfortable seat for the rider.

Structural Integrity

In order to maintain structural integrity of the sled the existing tunnel was left untouched and the battery box attached directly to the tunnel. Strength and weight were the two main considerations in selecting materials for battery box construction. Aluminum was selected because it provides the needed strength while being lighter than other materials.

To determine the structural soundness of the battery box, a simple stress analysis using elementary beam theory was performed to ensure that it would be able to hold the rider's weight. Based on the dimensions of the main support bar of the battery box, reaction forces were found followed by the maximum moment. These forces and moments were found using shear and moment diagrams similar to those in Figure 2. The maximum moment at the center of the bar, based on a 400 lbf loading on each side, was found to be 2.5 ksi. The yield strength of the aluminum is 8 ksi, resulting in a safety factor of 3.

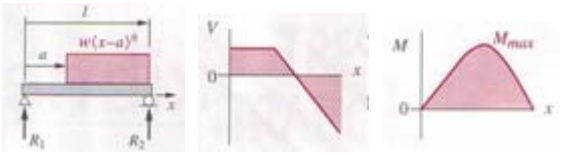

Figure 2: Shear and moment diagrams for a distributed loading.

A layer of undercoating was applied to the inside of the box structure in order to seal and make the box nonconductive. Fitting the box with foam provided an added measure to ensure the box was nonconductive. To provide ventilation for the batteries, the holes the battery wiring comes through were left unsealed.

Thermal Considerations

To predict the sled's performance during the cold start event, the batteries' temperatures need to be known. To simulate the conditions for the cold start event a transient heat analysis was performed. The Biot number was found using:

$$Bi = \frac{hc_{onv} \cdot L}{k}$$

The Biot number was too large to be able to use the Lumped Capacitance Method. The next step was to determine the Fourier Number.

$$Fo = \frac{\alpha \cdot L}{t^2}$$

The Fourier Number is greater than 0.2 so the Approximate Solution Method was used to calculate the final temperature, T_o. The approximate solution is found using:

$$\theta_o^* = c_4 \cdot e^{(-\zeta_1^2 * Fo)}$$

where

$$\theta_0^* = \frac{T_o - T_\infty}{T_i - T_\infty}$$

and c_4 and ζ_1 are coefficients based on the Biot number.

After eight hours with T_o = 70° F, the temperature inside the battery box would be the same as the ambient air, 32° F. Based on the battery operating temperature range, the sled is expected to pass the cold start event without problems.

In order to find the temperature of the battery box during continuous operation, an assumption that the battery box will reach a steady-state condition was used. To find the steady-state temperature, a thermal resistance network was created for the battery box. The total resistance of the battery box is:

$$R_{tot} = R_{cAl} + R_{cf} + R_{cv}$$

where

$$R_{cond} = \frac{L}{k \cdot Area}$$

and

$$R_{conv} = \frac{1}{h_{conv} \cdot Area}$$

Using the thermal resistance, the heat transfer rate can be found using:

$$q_{tot} = \frac{T_i - T_\infty}{R_{tot}}$$

Using an energy balance of:

$$E_{in} - E_{out} + E_{gen} = E_{st}$$

it was found that the heat flux of the batteries is equal to the heat out of the battery box, q_{tot}. Using this

information, the steady-state temperature of the battery box can be found.

Front Suspension

The front suspension of the 2005 Yamaha Vector was analyzed to calculate the adjustments and modifications required for the additional weight added to the rear of the sled as a result of the electric conversion. The major concern in making adjustments to the front suspension was the handling characteristics of the snowmobile. The adjustments that were made were done in an effort to make the converted sled handle like the stock sled.

Analysis

Analysis of the front suspension began with gaining a proper understanding of the existing stock suspension on the sled. The stock suspension is a four-bar non-Grashoff linkage with nitrogen gas charged shocks and coil springs. This information was important to understand how to begin a proper kinematic 4-bar linkage analysis. The lengths of each suspension component were measured and then used in the following equations to understand how the system would move.

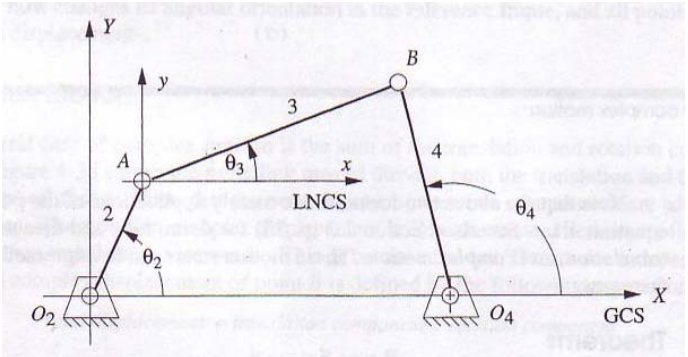

Figure 3: Free Body Diagram of kinematic analysis (Norton, 1999)

To begin the kinematic analysis, the lengths and angles of each suspension component were measured as shown in Figure 3.

$$a := 15.375in$$

$$b := 3.25in$$

$$c := 16.8125in$$

$$d := 3.25in$$

The following intermediate constants were then calculated:

$$K_1 := \frac{d}{a}$$

$$K_2 := \frac{d}{c}$$

$$K_3 := \frac{a^2 - b^2 + c^2 + d^2}{2 \cdot a \cdot c}$$

$$K_4 := \frac{d}{b}$$

$$K_5 := \frac{c^2 - d^2 - a^2 - b^2}{2 \cdot a \cdot b}$$

$$A(\theta_2) := \cos(\theta_2) - K_1 - K_2 \cdot \cos(\theta_2) + K_3$$

$$B(\theta_2) := -2 \cdot \sin(\theta_2)$$

$$C_.(\theta_2) := K_1 - (K_2 + 1) \cdot \cos(\theta_2) + K_3$$

$$D(\theta_2) := \cos(\theta_2) - K_1 + K_4 \cdot \cos(\theta_2) + K_5$$

$$E(\theta_2) := -2 \cdot \sin(\theta_2)$$

$$F(\theta_2) := K_1 + (K_4 - 1) \cdot \cos(\theta_2) + K_5$$

The values for theta are then:

$$\theta_3(\theta_2) := 2 \cdot \operatorname{atan}\left(\frac{-E(\theta_2) - \sqrt{E(\theta_2)^2 - 4 \cdot D(\theta_2) \cdot F(\theta_2)}}{2 \cdot D(\theta_2)} \right)$$

$$\theta_4(\theta_2) := 2 \cdot \operatorname{atan}\left(\frac{-B(\theta_2) - \sqrt{B(\theta_2)^2 - 4 \cdot A(\theta_2) \cdot C_.(\theta_2)}}{2 \cdot A(\theta_2)} \right)$$

$$\theta_s(\theta_2) := 0.5108058472 \theta_2^{1.0903773375}$$

Once finished, the kinematic analysis was followed by the solid modeling shown in Figure 4. Using the kinematic analysis and solid models, the suspension's physical limitations were found to only allow the pivot angle to range from 108.7° to 136.1°. The kinematic analysis was then followed by a free body diagram to show the forces in all of the suspension pieces including the force compressing the spring-dampener system. The results from the force analysis are shown in Figure 5. These results explain what adjustments were made to improve the overall static stance of the sled. The initial calculations assumed the nose weight of the sled to be 400lbs. This estimate was high, but was easily changed when the final weight was established.

Figure 4: Outline of the Front Suspension.

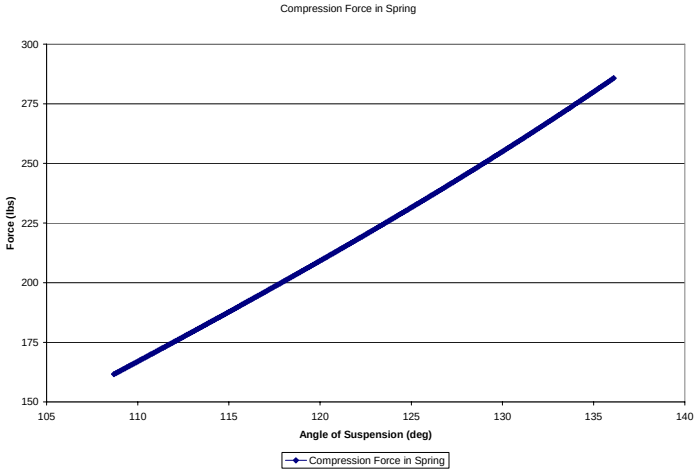

Figure 5: Compression Force of Spring vs. Angle of Suspension in degrees. The force in the spring dampener system is shown (individual side). The weight of the nose for this graph is 400 lbf. The pivot angle referenced in Figure 4 is shown.

Modifications and Adjustments

No Modifications are needed to the existing front suspensions system. The existing adjustability of the front suspension is all that is needed because the overall nose weight of the sled only varies slightly.

Rear Suspension

The Yamaha Vector came with a two-degree-of-freedom rear suspension. This separates the vertical movement from the tilt of the track, allowing for maximum traction and control on and off the trail. The rear suspension has a helical compression spring over a gas-charged shock in the front to control part of the vertical movement. The coil-over shock has an adjustable spring perch to allow change of the preload in the spring and a limiting strap to control its movement. The rear portion of the suspension has two helical torsion springs that control the tilt and the vertical movement in the track. The helical torsion springs are connected to adjustable cams, which help to control the tension in the springs.

Analysis and Modifications

The rider comfort is affected by the body roll of the sled. To keep the handling characteristics similar to a stock chassis, the rear suspension was modified. This was done by shortening the limiting straps and increasing the torque from the rear spring.

The stock track's main point of contact on dry ground is at the front of the track. This allows for excellent handling because the center of gravity is between the front of the track and the skis (see Figure 6). The stock setup allows for a balanced weight distribution.

Figure 6: Contact point and center of gravity of stock sled

The modified sled's center of gravity was pushed back behind the track's main point of contact on dry ground (see Figure 7). The modified sled became difficult to maneuver because the skis had little load on them.

Figure 7: Contact point and center of gravity of electric sled before modifications

The solution for keeping similar handling characteristics was to move the track's main point of contact on dry

ground back behind the modified center of gravity (see Figure 8).

Figure 8: Contact point and center of gravity of electric sled after modifications

This was done by shortening the limiting straps (see Figure 9). The shortened limiting straps pulled the front of the track up and moved the track's main point of contact to the rear of the sled. This increased the load on the skis for a balanced-weight distribution allowing for better sled control.

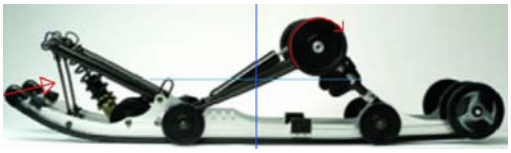

Figure 9: Effect of shortening limiting straps

To accommodate for the new mass of the sled, the stock rear-torsion springs were replaced with other Yamaha springs that were 31% stiffer. Also, new tensioning cams were built to increase the preload in the spring.

To find the new load applied to the rear link of the suspension, the angle of deflection on the stock spring was found when it was loaded with all the components. By summing the forces, the load from the sled was calculated to be 361 lbf on the rear link of the suspension based on the following equation:

$$L_{sled} = \frac{2 \cdot \tau_{cs}}{\delta_c \cdot \sin\left(\phi_c\right)}$$

where

$$\tau_{cs} = 142.76 \ ft \cdot lbf$$

$$\phi_c = 71.6 deg$$

$$\delta_c = 10 in$$

The necessary torque to keep the sled at stock height with a rider was calculated by:

$$\tau_{0f} = \delta_f \sin\left(\phi_f\right) \cdot \left(L_{sled} + W_{rider}\right)$$

From these equations, it was determined that the new cam height needed to be 2.5 in.

DRIVE-TRAIN

The drive-train team started its analysis with the goals of achieving 10 miles continuously running at 20 mph and being able to pull 1500 lbf over 100 ft. To achieve these goals, all components of the drive-train needed to be optimized together to produce the maximum possible efficiency. Beginning with motor selection and continuing with the drive system, this process is described below.

Motor Selection

Due to budget constraints, motor selection was limited to the two motors from the previous year. Both motors are Advanced DC Motors 203-06-4001. One of these motors runs strictly in series and the other is capable of running in either parallel or series. The decision of which motor and configuration to use comes by weighing the characteristics of one motor against the other.

Motor Testing

The motor testing was done with a Prony brake dynamometer. The controller's 72V DC output signal interfered with the data acquisition system and could not be processed. The tests were then performed without a controller at 24V DC and 48V DC for safety reasons. The key pieces of information obtained for comparison were: efficiency, torque output, and current draw.

These values are necessary for performing drive analysis and predicting range, acceleration, and top speed. The data obtained is quantified below, making reference to the motors in terms of the paint color on the motor.

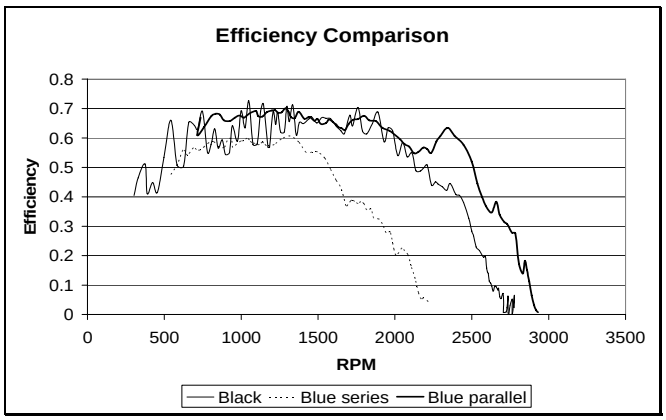

Figure 10: Efficiencies for the Motors at 24 volts

Figure 10 relates the efficiencies of the different motor configurations at 24V DC as a function of RPM. Note that the blue-parallel and black motors have similar efficiencies with peaks no greater than 70%; on average there is a 5% gain in efficiencies when run at 48V DC.

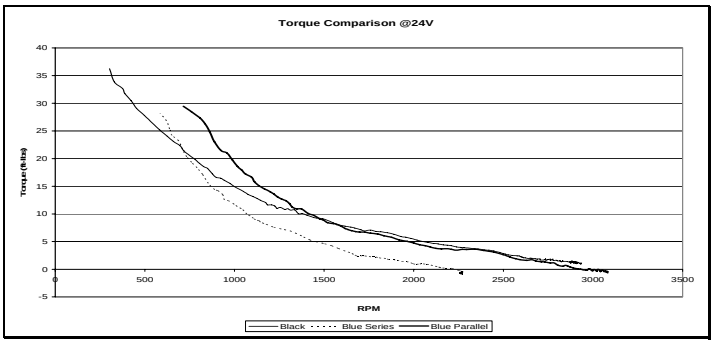

Figure 11: Torque Comparison at 24 volts

Looking at the torque comparison, the blue parallel and black motors are nearly identical above 1400 RPM. However, below 1400 RPM, the blue-parallel motor has a higher torque curve, which would give a slight advantage for the acceleration event. This boost however, comes at the price of current, as seen below in Figure 12.

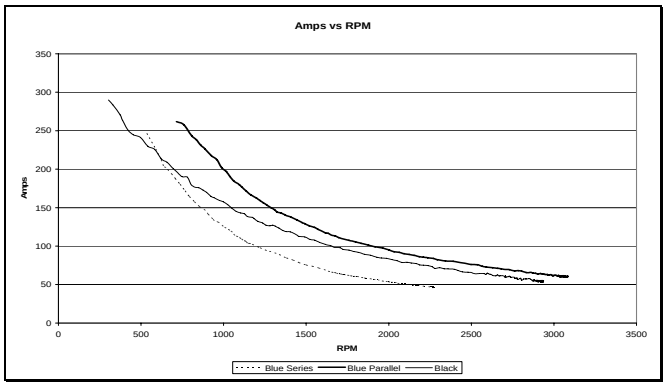

Figure 12: Ampere Draw at 24 Volts

All of this information must be considered when deciding which motor will be used to power the sled. The decision comes down to selecting the motor with the best efficiency and lowest current draw that will output enough torque to overcome mechanical losses. Judging from the data presented, the motor of choice is the black motor.

Motor Mount

Making the transition from an IC engine to an electric motor requires ingenuity when it comes to mounting. There are tight restraints on the motor due to the limited space in the compartment as well as the shaft alignments and center distances. It is preferred that the motor be restrained at both ends to prevent alignment issues. Another desired feature is the ability to tension the belt with the mount instead of incorporating a bulky idler pulley. Selecting the material for the motor mount was the next critical step. Ultimately 6061-T6 aluminum was chosen over steel for its light weight and cold temperature strength. Due to the lack of structure in the vector's engine compartment, it was decided to incorporate the stock mounting points into the design to cut down the weight of added supports. Integrating the stock-mount points is also beneficial to aligning the primary and secondary shafts. The mount was designed with a minimum safety factor of two assuming a peak torque of 120 ft*lbf with a belt pre-tension of 120 lbf on a 1-in-diameter pulley. The peak torque was extrapolated from the motor tests as a worst-case scenario.

Drive System

Drive Selection

In selecting a drive system for an electric snowmobile, there were three main drive types considered: a standard CVT, a synchronous belt drive, and a multi-V-belt drive. In order to choose a drive system, a decision matrix was used.

When selecting the transmission for the electric snowmobile, there were many concerns to address and many drive types to consider. The three main drive types to choose between were the standard CVT, a synchronous belt drive, and a multi-V-belt drive. Table 1 is a decision matrix that weighs the drive systems against each other. (5 = good and 1 = worst.)

Table1: Decision Matrix for the Drive System

	$	Efficiency	Weight	Startup Shock	Tot
Synchronous Belt Drive	5	5	4	2	16
Multi V-belt Drive	2	3	4	3	12
CVT	2	1	2	5	10

From Table 1 it is visible that the synchronous belt has the clear advantage over multi V-belt drives and the CVT. The cost savings comes from already having most of the infrastructure for this system.

Drive Ratios

The system chosen was directly driven by a single ratio because an automatic two-speed transmission would be too bulky. Finding the proper ratio had a profound effect on the performance and range of the sled. From the dynamometer tests, it was visible that the RPM of the peak efficiency did not coincide with the RPM of maximum power. This means that a single ratio will not be equally effective for acceleration and range. The major limitation of this electric snowmobile was and continues to be its range. This is where the most improvement is needed and thus the ratio was selected to increase the range.

This was done by relating the vehicle velocity, in RPM, through the track and chain case ratios to the desired operating RPM of the motor. This gave the drive ratio for maximum range. At 20 mph, and motor speed of 1300 RPM, the required ratio is .9:1. However, this ratio is pending further drag-test data to ensure that enough torque is transmitted to move the sled competitively. Moreover, it may be the case that the 10-mile competition goal can be achieved with a less-efficient ratio; in which case a ratio would be selected to yield more torque to improve acceleration and pulling power while maintaining a 10-mile range goal.

Incorporating the drag data with the motor characteristics and vehicle setup, it is possible to predict the acceleration and top speed of the vehicle. By using the following relationships, the governing equations of motion may be established.

The following equations are derived by coupling the free body diagram of the cogs in Figure 13.

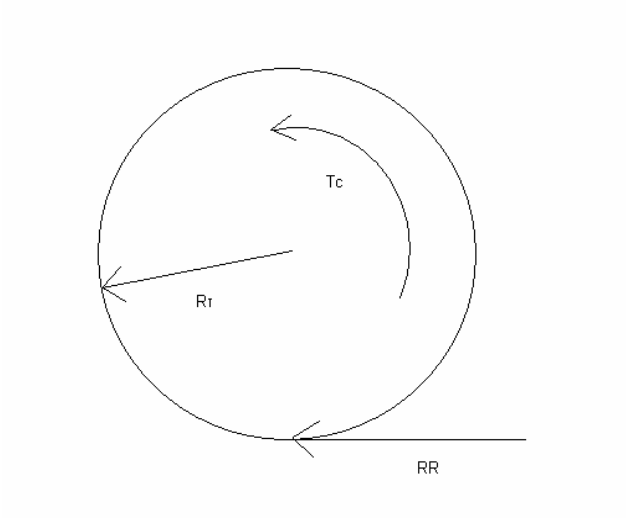

Figure 13: Free Body Diagram for the drive cogs

Combining Newton's and Euler's equations with Figure 13 provides the basis for the dynamic relationship seen below.

$$\frac{\tau_C}{R_\tau} - RR = m \cdot x'' + J \cdot \theta''$$

Assuming a no slip condition, the following relationships are established:

$$x = \theta \cdot R_\tau$$

$$x' = \theta' \cdot R_\tau$$

$$x'' = \theta'' \cdot R_\tau$$

Combining these equations, it is possible to provide a differential equation based in the x coordinate system. This equation is shown below.

$$x'' = \frac{1}{m + \frac{J_{equiv}}{R_\tau^{\,2}}} \cdot \left(\frac{\tau_m \cdot R_{ms} \cdot R_{sc} \cdot \frac{x'}{R_\tau} \cdot R_{ms} \cdot R_{sc}}{R_\tau} - RR \right)$$

Numerically solving the above equation will yield estimated times for the 100 ft acceleration event and give an idea of top speed for a variety of gear ratios. A distance vs. time graph is shown below for a selection of 5 speed ratios. For comparison, the average time for an electric sled at CSC 2006 was 17.5 seconds.

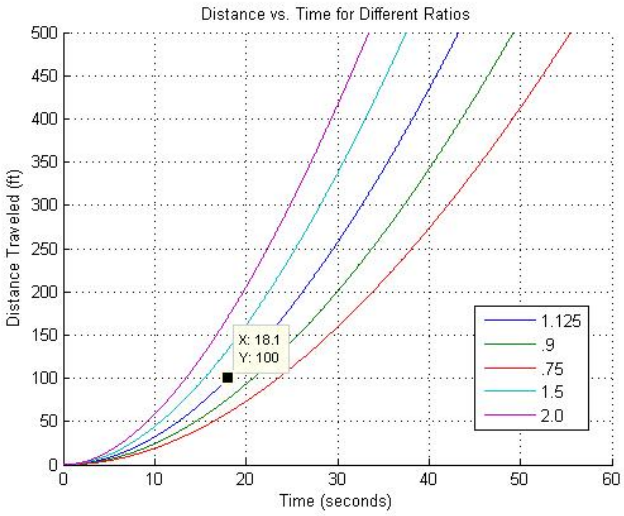

Figure 14: Distance vs Time for Different Loads

Comparing the acceleration results to the energy model estimates seen below, the 1.125 ratio is analytically the best ratio and will be the first one tested.

Table 2: Energy Model Estimates for Selected Ratios

R_{ms} (unitless)	Range @ 20 mph (miles)
0.75	6.3
0.9	6.5
1.125	6.61
1.5	6.37
2	4.3

ELECTRICAL SYSTEMS

The electrical team designed for efficiency, reliability, simplicity, and safety.

The efficiency goal of the electrical system coincided directly with the team's goal of a range of 10 miles at a continuous speed of 20 mph. Efficiency planning went into battery selection, battery layout, alternative low-power components, recharging, and system wiring.

The reliability of the electrical system is very important, especially for competition. In designing a more reliable electrical system, more unexpected problems will be reduced and troubleshooting will be easier. To make the vehicle more reliable, the electrical team designed the electrical system to be as simple as possible. This meant the electrical team needed to minimize elaborate electrical systems and reduce power losses to unnecessary components.

To make the sled user-friendly, an ammeter and voltmeter will indicate the drive system energy status. As an added feature, a built-in battery tester was designed into the system. This added feature will allow the user to diagnose each drive system battery independently by checking its voltage, as seen in Figure 15.

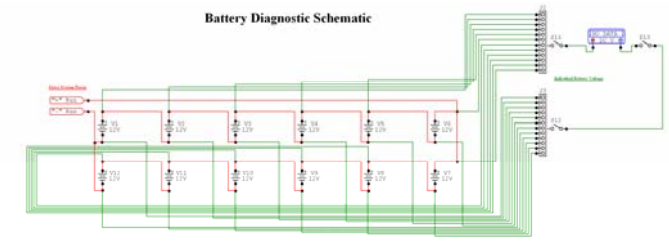

Figure 15: Battery Diagnostic Schematic

The challenge for meeting the ten mile competition requirement for the snowmobile is highly dependent on the efficiency of each component in the snowmobile. There are various electrical components on the snowmobile where it is important to optimize the efficiency.

A strategy was used for each component in order to choose the most efficient configuration for this snowmobile. The motor was mainly chosen due to financial constraints but was optimized to run in series.

The motor controller was chosen for a 72V DC circuit. The efficiency of the motor controller is fixed based on the characteristics of the controller itself. The controller was chosen based on our power requirements and financial constraints.

Another electrical efficiency variable is the vehicle's wiring layout. Wire of appropriate gauge must be used in order to deliver sufficient power to the drive system. With an expected current flow in excess of 100 Amps, the required wire gauge will have a noticeable increase in line resistance. Therefore, in order to reduce power loss due to wire resistance, wiring distances must be minimized. It is imperative to maintain the highest possible efficiency to increase the range of the snowmobile. Also, by designing the electrical system of the vehicle to be simple will further reduce efficiency losses. In order to conserve energy for the main drive system, an independent auxiliary electrical system is used. This system will be used to power basic snowmobile components such as lights, gauges and switches.

Battery Selection

Battery selection was the largest efficiency variable of the electrical system. In order to achieve the target range of 10 miles, it was desired to have a battery with the following criteria: low-cost, efficiency, a high energy density, and durability.

Initial intuition suggested that using the lead-acid battery technology would be unfavorable due to its high weight, lower energy density, and average low operating temperature. Other battery technologies were researched and analyzed in order to find the battery of choice.

The Lithium Ion batteries are the ideal battery technology because of their high energy density. Lithium ion technology, however, requires electronics to monitor their performance to prevent damage to the cells, which adds to the complexity of the electrical system. This was a large conflict with the team goal of reliability and simplicity.

The NiCd batteries have their own unique problem. Analysis showed that more than 100 DeWalt power-drill batteries would need to be wired together to meet the power requirements of the sled. Wiring this many batteries adds complexity and introduces more line

resistance. This takes away from keeping an efficient vehicle.

Another limitation, that has been previously mentioned, was the financial constraint. Lithium Ion batteries are currently the most expensive battery technology. Their price ranges from nearly five times more expensive than a lead-acid battery. Also, NiCd batteries are priced double of the same lead-acid batteries. After careful consideration of the batteries that made it through the first phase of design, a decision matrix, as seen in Figure 16, was created to show that the 12 V 55 AH lead-acid batteries would be in the sled for this year's competition.

Battery	technology	Brand	Volts	Amp-Hrs	lbs.	x	y	z	Watt-Hrs
#1	Lead Acid Gel	AGM	12	55	37.4	8.46	9.01	5.43	660
#2	Lead Acid Gel	PowerSonic	12	55	41.9	8.27	8.95	5.39	660
#3	NiCad	Dewalt	24	2	2.4	7.6	7.3	4.1	48
#4	Lead Acid Gel	PowerSonic	12	75	55.11	13.7	7	6.57	900
#5	Lithium Ion	Valence	12.8	130	40.9	8.8	12	8.8	1664

Battery	W/kg	# Series	# Parallel	# Total	Total lbs.	Sled W/kg	$/batt.	$ Total
#1	38.90510509	6	2	12	448.8	16.873416	$58.98	$707.76
#2	34.72675252	6	2	12	502.8	16.036564	$100.00	$1,200.00
#3	44.09245244	3	46	138	331.2	15.92174	$12.00	$1,656.00
#4	36.00383563	6	2	12	661.32	19.088866	$120.00	$1,440.00
#5	89.69418197	6	1	6	245.4	26.474564	$600.00	$3,600.00

Morph Chart		#1	#2	#3	#4	#5
cost	35%	5	3	3	3	1
size	5%	4	4	5	2	4
charge	10%	5	4	2	4	2
wining	5%	5	5	1	5	4
W/kg	35%	3	2	4	3	5
Efficiency	10%	2	2	4	2	5
Total	100%	3.95	2.8	3.35	3.05	3.2

Color Code Key
User Inputs
Calculated Values
Heading
Sub Heading

chassis lbs.	drive train lbs.	power lbs.	Total lbs.
0	586	448.8	1034.8

Designed Total Power	
Motor	72 Volts
	6600 Watts

Battery Selection		
#1	AGM	$707.76

Figure 16: Comparison and Selection of Researched Batteries

In summary, it was concluded that a high performance lead-acid battery would be the best choice for our application. The lead-acid battery is rugged enough to fully discharge without penalties like the other batteries that were analyzed. Also, they have the highest overcharge tolerance. As far as the low-end operating temperature of the lead-acid battery, they were found to be comparable to that of other battery technologies.

Safety

The safety of the user is of top importance in the overall design. In order to accomplish this, the electrical system is designed to allow the user to perform system diagnostics safely from an externally mounted diagnostics gauge. Also, during any form of maintenance, the electrical systems are equipped with directional, quick-disconnecting attachments. These will prevent the user from damaging the electrical system from improper hook up and protect the user from exposure to shock.

The vehicle is equipped with redundant power deactivation switches. These include the keyed switch, kill switch, and the tether chord. All switches must be in the closed position in order for the vehicle to operate. The keyed switch is to protect against vehicle theft, the kill switch is used for an emergency shut-down, and the tether chord is used in the event of the rider falling off.

Auxiliary System

In order to conserve the maximum amount of energy for the drive system, unnecessary power losses need to be eliminated. To achieve this, an auxiliary power system was designed. This system removes the burden of the drive system from powering the miscellaneous electronics common to a snowmobile. To minimize the power consumption of the auxiliary system, low power components were used where possible. Light Emitting Diodes (LED) replaces the running lights and the brake light. The main headlight assembly will still consist of halogen lamps but will be able to be switched off when not needed in order to conserve power. Figure 17 shows the diagram of this system.

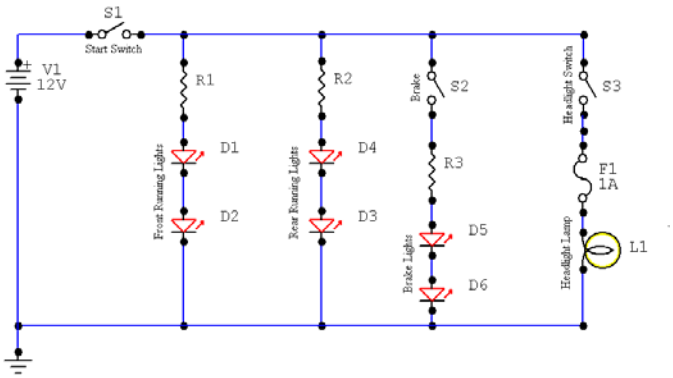

Figure 17: Auxiliary Power System

Main Electrical System

The main power system of the snowmobile consists of the 12 lead-acid batteries. These batteries are completely dedicated to the operation of the motor controller and motor. This layout will maximize the available power to the drive system, in turn giving the maximum possible range. As a safety issue, the starter relay will be controlled by the auxiliary system so that the rider is removed from being exposed to such high power. This means that the auxiliary system must last longer than the drive system in order for the vehicle to drive. In the event the auxiliary system was not able to last longer than the main system, the relay could be bypassed. For both the protection of the person and the

vehicle, this bypass is strongly discouraged. Figure 18 shows a schematic of the main electrical system.

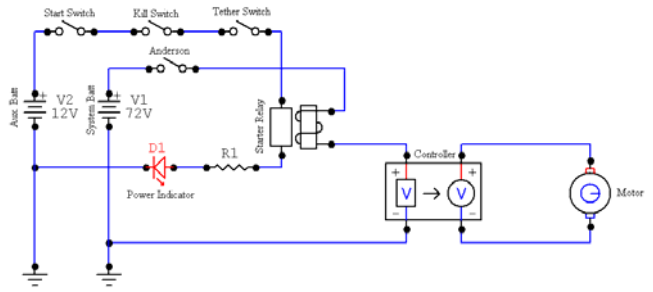

Figure 18: Schematic of Main Electrical System

Another method of increasing the efficiency of the main electrical system lies in the battery layout, as previously discussed. The system's high current draw mandates lower gauge wire to be used. Lower gauge wire has an increase in line resistance per unit length. Minimizing wire length is a necessary design issue that was taken into account so as to reduce power loss as much as possible. Figure 19 shows the top view of the battery layout and how the batteries are wired.

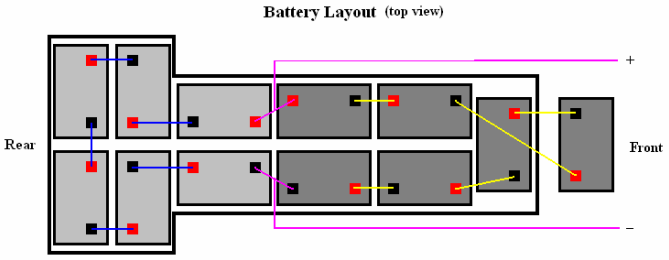

Figure 19: Top View of Battery Layout

SUMMARY OF ENERGY MODEL

The objective of the energy model is to predict how far the Zero-Emission Utah State Snowmobile (ZEUS) will travel given a charge with its twelve lead-acid batteries. The distance to be traveled is a function of elevation increase, mass of the sled and rider, and velocity of the sled.

Solution to Distance Traveled

Velocity of the sled and motor RPM are directly related due to the direct-drive transmission. To find the motor RPM from the velocity in miles per hour, the following formulas were used. Similarly, velocity was calculated for a given motor RPM.

$$RPM = \frac{60 V_{fts}}{d_{equiv} \cdot \pi} \cdot R_g \cdot R_{ms}$$

where

$$V_{.fts} = c_{.1} \cdot V_{.mph}$$

and

$$c_{.1} = 1.467$$

The total distance the sled will travel is limited by the amount of drag that the sled creates as it maintains zero acceleration at operating speeds. The greater the rolling resistance, the larger the other component inefficiencies become. A drag test on the 2007 ZEUS provided the following data:

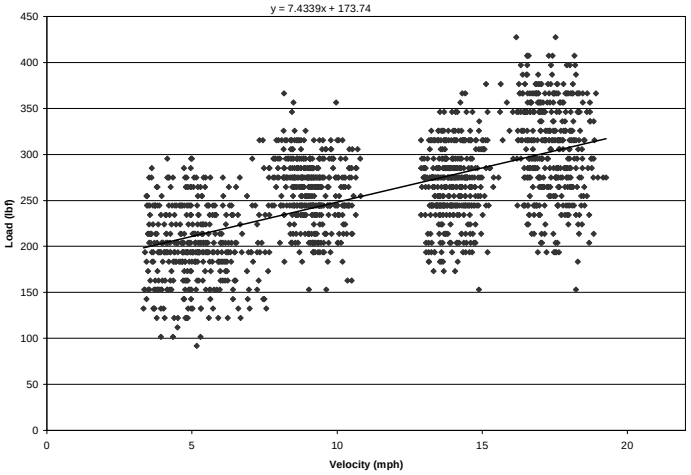

Figure 20: Rolling Resistance (lbf) Vs Velocity (mph)

From this data, the total amount of motor torque can be calculated by:

$$\tau_M = \frac{RR \cdot R_\tau}{\eta_t \cdot R_{sc} \cdot R_{ms}}$$

where

$$R_{ms} = 1.125$$

$$R_{sc} = 1.75$$

$$R_{\tau} = 0.292ft$$

and the transmission efficiency is assumed to be:

$$\eta_t := 0.97$$

The amount of current used by the motor to produce a given amount of torque is given from data from the manufacturer. This data was not tested experimentally due to safety concerns of using a 72V DC circuit. Figure 21 shows the data along with a linear-fit regression analysis of current versus motor torque.

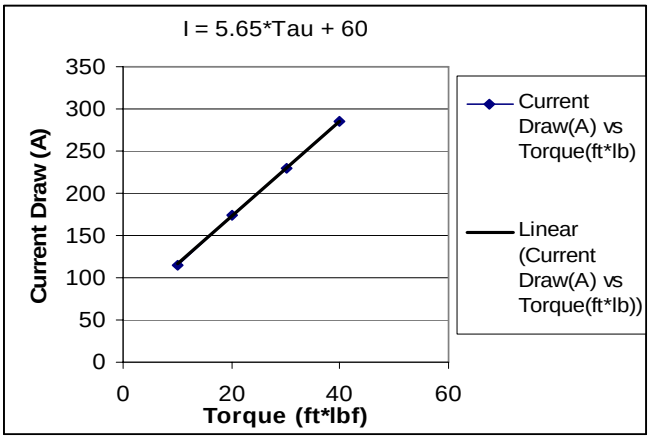

Figure 21: Current Draw (A) Vs Motor Torque (ft*lbf)

Internal battery resistance is a function of operating temperature of the battery. Operating temperature is a function of the ambient air temperature of the battery box. The 2005-2006 team measured the steady-state temperature inside the battery box at 70 degrees Fahrenheit during use. The room temperature resistance of 0.01 Ohms, published by the manufacturer and verified experimentally, was used in this analysis. To find the equivalent resistance of the battery pack combination (two packs of six batteries in series, connected in parallel), the following formula was used:

$$\frac{1}{R_{bequiv}} = \frac{1}{6 \cdot R_b} + \frac{1}{6 \cdot R_b}$$

Battery efficiency is then calculated by:

$$\eta_b = \frac{E_0 - R_{bequiv} \cdot I}{E_0}$$

The efficiencies of the motor and controller were measured together experimentally in a dynamometer test. Results from this test are shown in Figure 22.

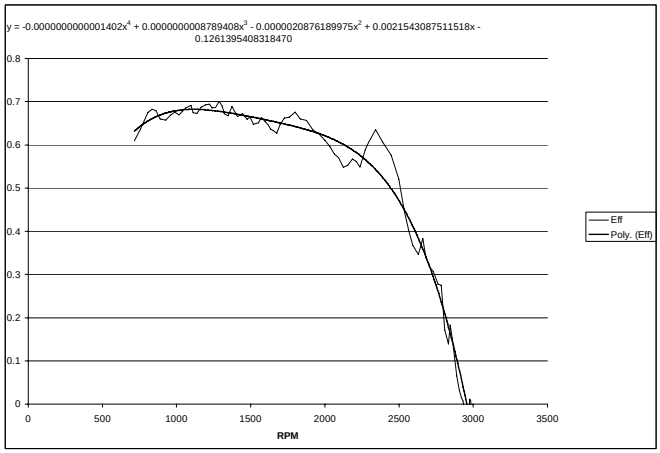

Figure 22: Motor and Transmission Efficiency Vs Motor RPM

The total component efficiency is then calculated by:

$$\eta_{Tot} = \eta_b \cdot \eta_c \cdot \eta_m \cdot \eta_t$$

where controller efficiency is assumed to be:

$$\eta_c = 0.95$$

In order to solve for the distance the sled will travel, the unit convention must be consistent. Total energy will be converted into lb*ft units by:

$$T_{0Eng} = c_2 \cdot T_{0Si}$$

where

$$c_2 = 2.655 \times 10^6$$

and with 12, 55-AH, 12-V batteries:

$$T_{0Si} = 7.92kW \cdot hr$$

All variables for the steady-state approximation are now known. The distance that the sled will travel in miles is given by:

$$d = c_3 \cdot d_{ft}$$

where

$$c_3 = 1.894 \times 10^{-4}$$

and

$$d_{ft} = \frac{\eta_{Tot} \cdot T_{0Eng} - \frac{1}{2} m \cdot v_{fts}^{2} - mgh}{RR}$$

Total distance for given velocities in miles per hour in shown below in Figure 23.

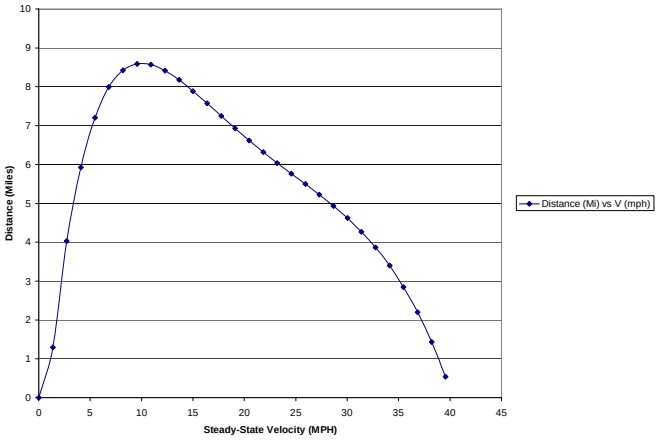

Figure 23: Total Distance Traveled at Given Velocities

CONCLUSION

This design paper discussed the conversion of a 2005 Yamaha Vector into a zero-emission snowmobile. There were many considerations taken into account in order to have a well handling, comfortable, and efficient sled ready for the SAE Clean Snowmobile Challenge. The analysis for the design decisions were thoroughly discussed throughout this paper. The chassis team took into consideration the handling characteristics and structural safety. These considerations were implemented into the design of the battery box and the front and rear suspensions. The drive-train team optimized the components of the drive system in order to achieve the goals of a 10-mile range at 20 mph and pulling 1500 lbf over 100 ft. A dynamometer test was performed to gather the data that determined the black motor would be the best choice to use for the competition. The electrical team designed for efficiency, reliability, simplicity, and safety. This was accomplished by designing redundant systems that would be familiar to an average snowmobiler and by cutting energy losses wherever possible. An energy model was developed to calculate the distance that the snowmobile would travel on a given charge assuming constant velocity and steady-state conditions. This energy model also helped the drive-train team select the optimum gear ratio.

ACKNOWLEDGMENTS

The 2006-2007 electric snowmobile design team would like to thank the following: Dr. Byard Wood, Dr. Ralph Haycock, and all of the generous university and faculty sponsors.

REFERENCES

1. Norton, R. L., *Design of Machinery*, 2nd ed., McGraw Hill, New York, 1999.
2. Norton, R. L., *Machine Design*, 3rd ed., Worcester Polytechnic Institute, Worcester, MT, 2006.
3. Incropera, F. P. and Dewitt, D. P., *Fundamentals of Heat and Mass Transfer*, 5th ed., John Wiley & Sons, Inc., New York, 2002.